Production of fragments with more neutrons than the projectile at intermediate energies

X. H. Zhang*
Institute of Modern Physics, Chinese Academy of Sciences, Lanzhou 730000, China
(Received 13 January 2015; revised manuscript received 4 February 2015; published 3 March 2015)

The nuclear reaction mechanism leading to the production of fragments with more neutrons than the projectile at intermediate energies is studied. A large enhancement in the production of these fragments is observed in the reactions with less neutron-rich projectiles or neutron-rich targets. This enhancement would be related to the difference of the neutron density at the nuclei surface as a factor influencing the process of nucleon exchange in peripheral collisions. From a practical viewpoint, such a nuclear reaction mechanism could provide a novel synthetic avenue to access extremely neutron-rich isotopes towards the neutron drip line.

DOI: 10.1103/PhysRevC.91.037602 PACS number(s): 25.70.Hi, 29.38.Db

I. INTRODUCTION

Exploration of the nuclear landscape towards the neutron drip line is currently of great interest in nuclear physics and astrophysics [1–5], and the efficient production of very neutron-rich fragments is becoming a key issue in current and future rare isotope beam facilities around the world [6–12]. In addition to the widely used target spallation, fission, and projectile fragmentation approaches, the search for new produced approaches is of exceptional importance.

At intermediate energies (40–200 MeV/nucleon), some neutron-rich fragments with more neutrons than the projectile have been observed [13–20]. The experimental results [18] showed that the velocities of these fragments are very close to the projectile velocity, and the production cross sections weakly depends on the projectile energy. As the velocities of these fragments are high enough to allow efficient collection and separation in practical applications, the production mechanism of these fragments could offer possible approaches to produce extremely neutron-rich isotopes towards the neutron drip line.

The nuclear reaction mechanism leading to the production of these fragments at intermediate energies has been described theoretically using the binary deep inelastic process [21]. The dynamics of the binary deep inelastic process is considered as the diffusive multinucleon transfer between the interacting nuclei in the peripheral collisions when the excitation energy of the produced exotic isotope is lower than the threshold for the neutron emission. The agreement of the model calculated results with the experimental data shows that this model seems to be able to explain the production of these fragments.

In recent years, some projectile fragmentation experiments using facilities at intermediate energies [10–12] have been done, and more experimental data of the fragments with larger neutron number than the projectile are available. In this paper, the production mechanism of these fragments will be further studied.

*zhxh@impcas.ac.cn

II. DATA AND DISCUSSION

The fragment momentum distributions provide valuable information about the reaction mechanism. In Figs. 1(a) and 1(b) the longitudinal momentum distribution peaks of the fragments with neutron number $N_f = N_p + 1$ and $N_f = N_p + 2$ are shown as a function of removed nucleons, $A_p - A_f$, respectively. Here N_f and A_f mean the neutron number and mass number of the target, and N_p and A_p are the neutron number and mass number of the projectile. The data are adopted from the reactions of ^{40}Ar at 57 MeV/nucleon [19], ^{40}Ca, ^{48}Ca, and ^{58}Ni at 140 MeV/nucleon [20] on ^{9}Be and ^{181}Ta targets. It is very clear that the velocities of both the fragments with neutron number $N_f = N_p + 1$ and $N_f = N_p + 2$ are very close to the projectile velocity, and the mass numbers of these fragments are close to the projectile mass. These facts indicate that this nuclear reaction must take place in the peripheral collisions and in a very short time. The prefragments will have low excitation energies due to the small difference between the velocities of fragment and projectile. The production of these fragments with more neutrons than the projectile must proceed via a transfer mechanism as described in Ref. [21], rather than via a deep inelastic collision in the low energy region leading to the transfer of a few neutrons and sizable velocity damping.

The production cross sections of these fragments as mentioned in Fig. 1 are plotted in Fig. 2 as a function of removed nucleons. The data of the fragments with neutron number $N_f = N_p + 1$ and $N_f = N_p + 2$ are shown in Fig. 2(a) and 2(b), respectively. It can be seen that for all the reaction systems the fragment cross sections decrease with the increase of the removed nucleons, and the maximum cross sections for the fragments with neutron number $N_f = N_p + 1$ and $N_f = N_p + 2$ are located around $A_p - A_f = 0$ and $A_p - A_f = -1$, respectively. With the increase of the removed nucleons by means of abrasion or exchange process in the collisions, the prefragment excitation energy will become larger. This would cause the decrease of the production cross section because of the deexcitation by neutron emission. Additionally, a weak dependence of the production cross sections on the projectile energy is observed in the reactions with neutron-rich ^{40}Ar projectiles at 57 MeV/nucleon and ^{48}Ca projectiles at 140 MeV/nucleon. This result is consistent with the

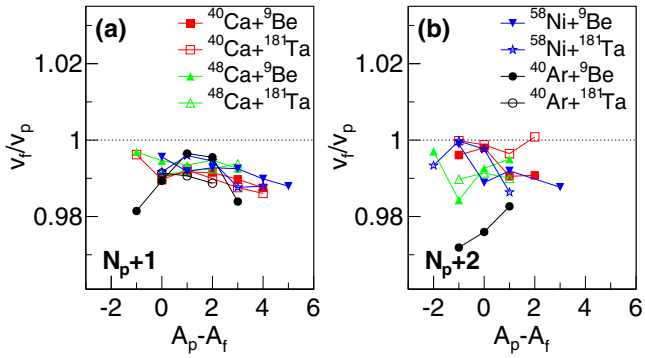

FIG. 1. (Color online) Longitudinal momentum distribution peaks of the fragments with neutron number $N_f = N_p + 1$ (a) and $N_f = N_p + 2$ (b).

conclusion in Ref. [18] and can be explained with the theory in Ref. [21].

In particular, the projectile and target dependance of the production cross section can be observed in Fig. 2. For a given reaction target, the cross sections of these fragments are obviously enhanced in the reactions with less neutron-rich ^{40}Ca and ^{58}Ni projectiles compared to the ones with neutron-rich ^{40}Ar and ^{48}Ca projectiles. For the reaction with a specific projectile, more fragments are produced in the reactions with the heavy target ^{181}Ta compared to the ones with the ^{9}Be target. According to Ref. [21], in the collisions a short-living dinuclear system (DNS) is probably formed in which the diffusion of nucleons occurs. So, the details of neutron and proton density profiles at the projectile and target surfaces would influence the process of the nucleon exchange just like the situations happening in the Fermi energy region. A large enhancement in the production of neutron-rich projectile residues has been observed in the reactions of a 25 MeV/nucleon ^{86}Kr beam with the neutron-rich ^{124}Sn and ^{64}Ni targets relative to the reaction with the less neutron-rich ^{112}Sn target [22], and the simulated results with a modified model of deep-inelastic transfer [23] indicated that the enhanced production of neutron-rich isotopes is associated with peripheral nucleon exchange in which the neutron skins of the neutron-rich target nuclei may play an important role [22,24]. When two nuclei come in contract, the exchange of nucleons may occur through

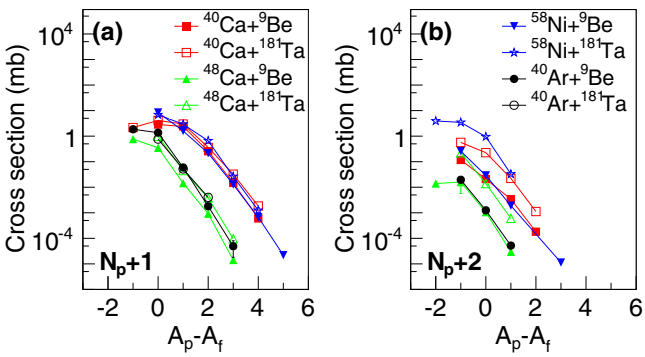

FIG. 2. (Color online) Production cross sections of the fragments with neutron number $N_f = N_p + 1$ (a) and $N_f = N_p + 2$ (b).

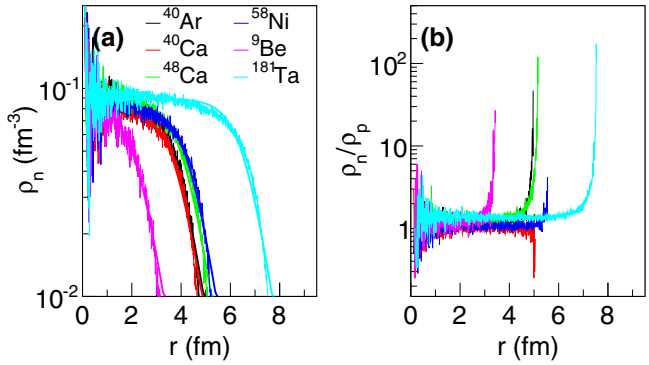

FIG. 3. (Color online) Neutron density distributions (a) and the ratios between neutron and proton densities (b) calculated with the HIPSE model. The solid curves in (a) are the fit results by using Eq. (1).

two processes [25,26]: one is isospin "drift" which causes the migration of neutrons from the high-density region to the low-density region, and the other is isospin "diffusion" which results in a migration of neutrons from the high N/Z region to the low N/Z region.

To understand whether the properties of nuclear surface influence on the cross sections, the neutron and proton density distributions of ^{40}Ca,^{48}Ca,^{58}Ni,^{40}Ar,^{9}Be, and ^{181}Ta have been calculated using the heavy-ion phase space exploration (HIPSE) model [27]. In HIPSE, the numerical method developed in Ref.[28] adapted to the Seyler-Blanchand parametrization of the force derived in Ref. [29] is used to calculate the realistic density distribution. Figure 3(a) shows the calculated neutron density distributions of these nuclei. In order to compare the neutron density at the nuclei surface, the neutron density distributions have been fitted with a Fermi -type density distribution [30],

$$\rho_n(r) = \frac{\rho_n^0}{1 + \exp\left(\frac{r - r_n^0}{d_n}\right)}, \tag{1}$$

where ρ_n^0 means the normalization constant, d_n is the diffuseness parameter, and r_n^0 is the radius of the half density for the neutron density distribution. Since the surface thickness of the stable nuclei is constant, the diffuseness parameter was fixed to 0.54 fm in the fitting [30]. The solid curves in Fig. 3(a) represent fits with Eq. (1), and the fitted numerical values are listed in Table I.

TABLE I. Values of the normalization constants and neutron radius calculated with the HIPSE model. The errors originate from the fittings.

	ρ_n^0 (fm^{-3})	r_n^0 (fm)
^{40}Ca	0.0806 ± 0.0005	3.8007 ± 0.0193
^{58}Ni	0.0827 ± 0.0005	4.3478 ± 0.0182
^{40}Ar	0.0862 ± 0.0005	3.8229 ± 0.0173
^{48}Ca	0.0883 ± 0.0005	4.1219 ± 0.0182
^{9}Be	0.0834 ± 0.0011	2.2165 ± 0.0259
^{181}Ta	0.0890 ± 0.0003	6.5842 ± 0.0169

Since the diffuseness parameter is a constant for all the nuclei in the fitting, the normalization constant can reflect the neutron density at the nuclei surface according to Eq. (1). From the Table I, it is clear that the neutron densities at the nuclei surfaces of the ^{40}Ar and ^{48}Ca projectiles are larger than that of the ^{40}Ca and ^{58}Ni projectiles, and the neutron densities at the nuclei surfaces of the ^{181}Ta target are larger than those of the ^{9}Be target. Due to the isospin drift, in the DNS the ^{40}Ca and ^{58}Ni projectiles with low neutron densities at the surface make it easier to pick the neutron from the target than the ^{40}Ar and ^{48}Ca projectiles, and the ^{181}Ta target with high neutron densities at the surface makes it easier to transfer the target neutrons to the projectile than the ^{9}Be target. The ratios between the neutron and proton density calculated with the HIPSE model are shown in Fig. 3(b). It can be seen that the influence of the nucleon exchange through the isospin diffusion process is similar to the isospin drift one.

The results calculated by HIPSE model indicated that the neutron density profiles at the nuclear surface would influence the process of nucleon exchange in the collisions, and result in a large enhancement of the production of fragments with larger neutron number than the projectile in reactions with less neutron-rich projectiles or neutron-rich targets.

As an example, the production cross sections of some neutron-rich fragments with neutron number $N_f = 29$ and $N_f = 30$ are plotted in Figs. 4(a) and 4(b) as a function of the fragment proton number Z_f. The solid circles are the experimental cross sections in the reaction ^{48}Ca $+^{9}$ Be at 140 MeV/nucleon [20], and the open circles, open squares, and open triangles show the cross sections of fragmentation of ^{54}Cr, ^{56}Fe, and ^{64}Ni projectiles in a ^{238}U target calculated with the EPAX 3 [31] model. To obtain larger cross sections, the projectiles which are close to these fragments and the very neutron-rich reaction target have been chosen in the calculations. However, the calculations are still tens of times smaller than the experimental data, even for the less neutron-rich target ^{9}Be used in the experiment. Considering the larger cross sections and high velocities, this transfer reaction would provide very efficient approaches for producing some extremely neutron-rich isotopes in the intermediate energy projectile fragmentation facilities. For practical purposes, the neutron-rich targets should be chosen in the planning of future experiments.

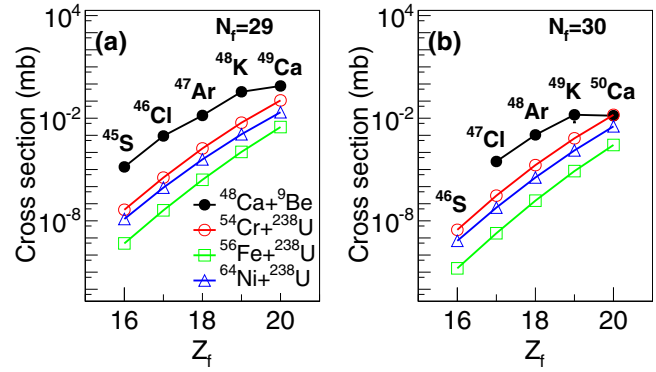

FIG. 4. (Color online) Production cross sections for $N_f = 29$ (a) and $N_f = 30$ (b) isotones. The experimental cross sections in the reaction ^{48}Ca $+^{9}$ Be at 140 MeV/nucleon [20] are shown by solid circles. Open circles, open squares, and open triangles represent the results of fragmentation of ^{54}Cr, ^{56}Fe, and ^{64}Ni projectiles in a ^{238}U target calculated with the EPAX 3 model.

III. SUMMARY

In this paper, the production mechanism of fragments with larger neutron number than the projectile has been studied at intermediate energies. The experimental data showed that this nuclear reaction must take place in the peripheral collisions and that the prefragments will have low excitation energies. A large enhancement in the production of these fragments in the reactions with less neutron-rich projectiles or neutron-rich targets is observed. This enhancement would be explained with the difference of the neutron density at the nuclei surface as a factor influencing the process of nucleon exchange. This reaction mechanism could offer a profitable pathway to produce extremely neutron-rich isotopes towards the neutron drip line at intermediate energies.

[1] R. F. Casten and B. M. Sherrill, Prog. Part. Nucl. Phys. **45**, S171 (2000).
[2] C. Sneden and J. J. Cowan, Science **299**, 70 (2003).
[3] K. Langanke and M. Wiescher, Rep. Prog. Phys. **64**, 1657 (2001).
[4] P. Danielewicz, R. Lacey, and W. G. Lynch, Science **298**, 1592 (2002).
[5] T. Sil, J. N. De, S. K. Samaddar, X. Vinas, M. Centelles, B. K. Agrawal, and S. K. Patra, Phys. Rev. C **66**, 045803 (2002).
[6] D. Habs, D. Rudolph, O. Kester, P. Thirolf, P. Reiter, D. Schwalm, G. Walter, P. V. Duppen, and J. Eberth, Z. Phys. A **358**, 161 (1997).
[7] J. R. Beene, D. W. Bardayan, A. G. Uribarri, C. J. Gross, K. L. Jones, J. F. Liang, W. Nazarewicz, D. W. Stracener, B. A. Tatum, and R. L. Varner, J. Phys. G **38**, 024002 (2011).
[8] R. Anne, D. Bazin, A. C. Mueller, J. C. Jacmart, and M. Langevin, Nucl. Instrum. Methods A **257**, 215 (1987).
[9] H. Geissel *et al.*, Nucl. Instrum. Methods B **70**, 286 (1992).
[10] B. M. Sherrill, D. J. Morrissey, J. A. N. Jr., and J. A. Winger, Nucl. Instrum. Methods B **56-57**, 1106 (1991).
[11] T. Kubo, M. Ishihara, N. Inabe, H. Kumagai, I. Tanihata, K. Yoshida, T. Nakamura, H. Okuno, S. Shimoura, and K. Asahi, Nucl. Instrum. Methods B **70**, 309 (1992).
[12] Z. Sun, W. L. Zhan, Z. Y. Guo, G. Xiao, and J. X. Li, Nucl. Instrum. Methods A **503**, 496 (2003).
[13] D. Guillemaud-Mueller, Yu. E. Penionzhkevich, R. Anne, A. G. Artukh, D. Bazin, V. Borrel, C. Détraz, D. Guerreau, B. A. Gvozdev, J. C. Jacmart, D. X. Jiang, A. M. Kalinin, V. V. Kamanin, V. B. Kutner, M. Lewitowicz, S. M. Lukyanov, A. C. Mueller, N. Hoai Chau, F. Pougheon, A. Richard, M. G. Saint-Laurent, and W. D. Schmidt-Ott, Z. Phys. A **332**, 189 (1989).

[14] M. Lewitowicz *et al.*, Phys. Lett. B **332**, 20 (1994).
[15] M. Notani *et al.*, Phys. Lett. B **542**, 49 (2002).
[16] G. A. Souliotis, D. J. Morrissey, N. A. Orr, B. M. Sherrill, and J. A. Winger, Phys. Rev. C **46**, 1383 (1992).
[17] R. Pfaff, D. J. Morrissey, M. Fauerbach, M. Hellstrom, J. H. Kelley, R. A. Kryger, B. M. Sherrill, M. Steiner, J. S. Winfield, J. A. Winger, S. J. Yennello, and B. M. Young, Phys. Rev. C **51**, 1348 (1995).
[18] S. Lukyanov, F. de. Oliveira. Santos, C. Borcea, G. Adamyan, M. Assie, R. Astabatyan, R. Borcea, A. Buta, L. Caceres, G. Georgiev, S. Grevy, M. N. Harakeh, O. Kamalou, M. Lewitowicz, V. Maslov, M. Mocko, Y. Penionzhkevich, L. Perrot, R. Revenko, F. Rotaru, M.-G. Saint-Laurent, M. Stanoiu, C. Stodel, J.-C. Thomas, B. M. Tsang, and P. Ujic, J. Phys. G **37**, 105111 (2010).
[19] X. H. Zhang, Z. Y. Sun, R. F. Chen, Z. Q. Chen, Z. Y. Guo, J. L. Han, Z. G. Hu, T. H. Huang, R. S. Mao, Z. G. Xu, M. Wang, J. S. Wang, Y. Wang, G. Q. Xiao, H. S. Xu, X. H. Yuan, H. B. Zhang, X. Y. Zhang, and T. C. Zhao, Phys. Rev. C **85**, 024621 (2012).
[20] M. Mocko, M. B. Tsang, L. Andronenko, M. Andronenko, F. Delaunay, M. Famiano, T. Ginter, V. Henzl, D. Henzlová, H. Hua, S. Lukyanov, W. G. Lynch, A. M. Rogers, M. Steiner, A. Stolz, O. Tarasov, M.-J. van Goethem, G. Verde, W. S. Wallace, and A. Zalessov, Phys. Rev. C **74**, 054612 (2006); M. Mocko, Ph.d. dissertation, NSCL/MSU, 2006 (unpublished), http://groups.nscl.msu.edu/nscl_library/Thesis/Mocko,%20Michal.pdf
[21] G. G. Adamian, N. V. Antonenko, S. M. Lukyanov, and Y. E. Penionzhkevich, Phys. Rev. C **78**, 024613 (2008).
[22] G. A. Souliotis, M. Veselsky, G. Chubarian, L. Trache, A. Keksis, E. Martin, D. V. Shetty, and S. J. Yennello, Phys. Rev. Lett. **91**, 022701 (2003).
[23] L. Tassan-Got and C. Stephan, Nucl. Phys. A **524**, 121 (1991).
[24] M. Veselsky and G. Souliotis, Nucl. Phys. A **765**, 252 (2006).
[25] V. Baran, M. Colonna, M. Di Toro, M. Zielinska-Pfabé, and H. H. Wolter, Phys. Rev. C **72**, 064620 (2005).
[26] J. Rizzo, M. Colonna, V. Baran, M. D. Toro, H. H. Wolter, and M. Zielinska-Pfabe, Nucl. Phys. A **806**, 79 (2008).
[27] D. Lacroix, A. Van Lauwe, and D. Durand, Phys. Rev. C **69**, 054604 (2004).
[28] D. Lacroix and P. Chomaz, Nucl. Phys. A **636**, 85 (1998).
[29] W. D. Myers and W. J. Swiatecki, Nucl. Phys. A **601**, 141 (1996).
[30] A. Ozawa, T. Suzuki, and I. Tanihata, Nucl. Phys. A **693**, 32 (2001).
[31] K. Summerer, Phys. Rev. C **86**, 014601 (2012).